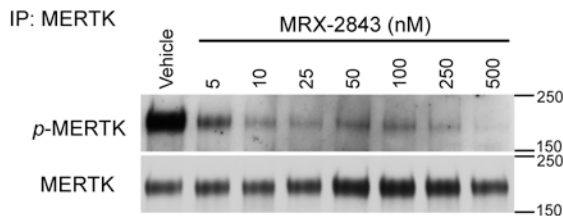# Supplemental Figures and Figure Legends
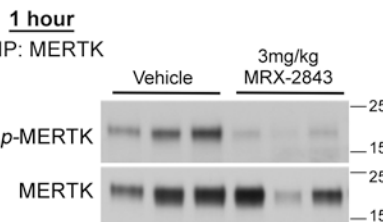
Supplemental Figure 1
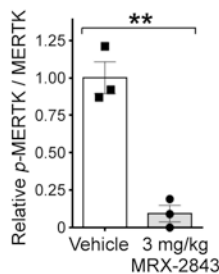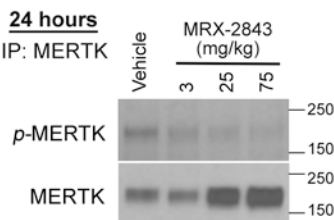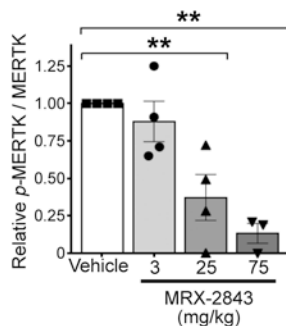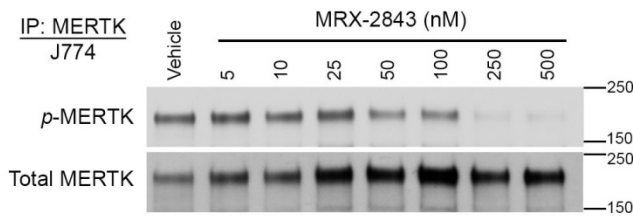

Supplemental Figure 1: Inhibition of MERTK using MRX-2843. (A) 697 cells were treated with vehicle (DMSO) or MRX-2843 for one hour and pervanadate phosphatase inhibitor was added to the cultures for three minutes to stabilize phosphorylated proteins. MERTK was immunoprecipitated from cell lysates and phosphorylated (denoted by p-) and total MERTK proteins were detected by immunoblot. (B-E) 697 cells were inoculated into NOD-SCID-gamma (NSG) mice by tail vein injection. After 14 days, mice with advanced leukemia were treated with a single dose of MRX-2843 or an equivalent volume of vehicle (saline). Femurs were harvested one hour (B-C) or 24 hours (D-E) after treatment and bone marrow cells were flushed with medium containing FBS and pervanadate phosphatase inhibitor. Human MERTK was immunoprecipitated from cell lysates and phosphorylated (denoted by p-) and total MERTK proteins were detecte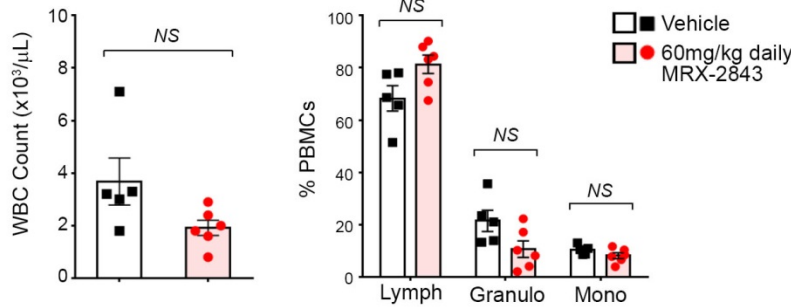d by immunoblot. Proteins were quantitated by densitometry and ratios of phosphorylated and total MERTK were calculated relative to vehicle-treated controls. Representative immunoblots are shown and mean values and standard errors are graphed (**$p<0.01$, 1-way ANOVA, n = 3-4).
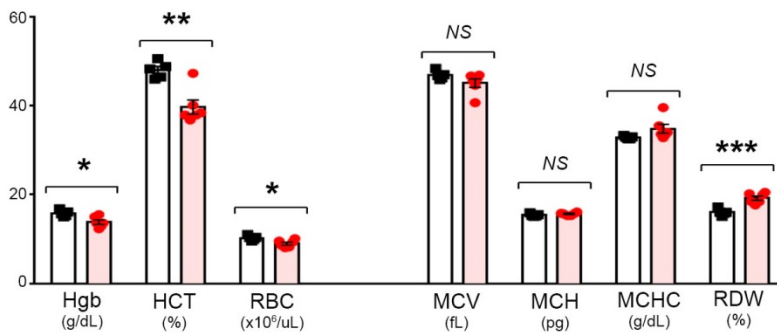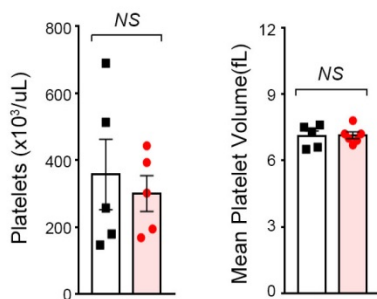
Supplemental Figure 2

A

B

C

D

E

Supplemental Figure 2: MRX-2843 inhibits murine MERTK and decreases bone marrow cellularity. (A) J774 cells were treated with MRX-2843 or vehicle for one hour and pervanadate phosphatase inhibitor was added to the cultures for three minutes to stabilize phosphorylated proteins. MERTK was immunoprecipitated from cell lysates and phosphorylated (denoted by p-) and total MERTK were detected by immunoblot. (B-E) Wild-type C57BL/6 mice were treated with 60mg/kg MRX-2843 or an equivalent volume of vehicle (saline) once daily for 24 days. Bone marrow from femurs and tibia and peripheral blood were collected. Complete blood counts were determined on peripheral blood samples. (B) Peripheral white blood cell (WBC) counts and differential (inc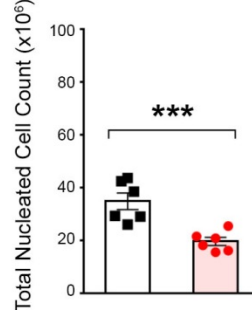luding percentages 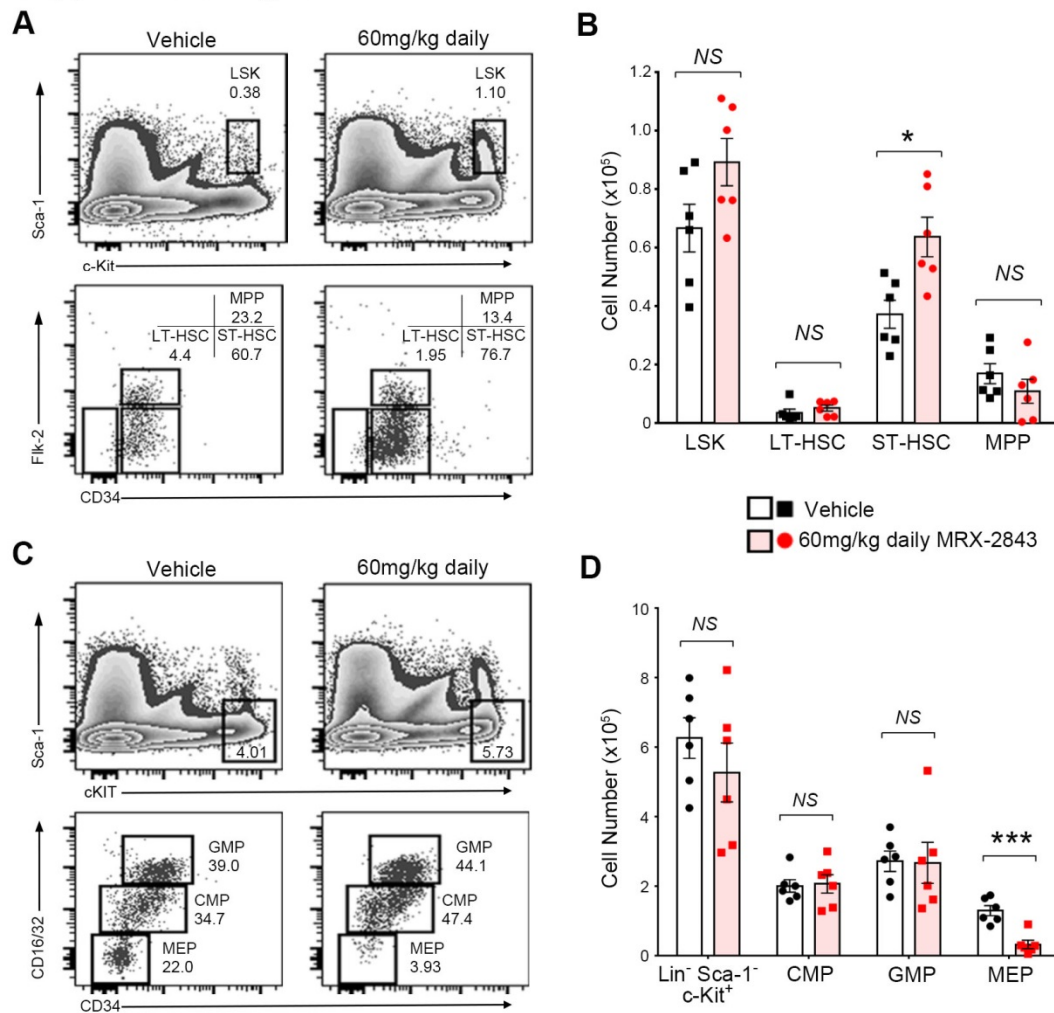of lymphocytes, granulocytes and monocytes) in peripheral blood mononuclear cells. (C) Red blood cell indices (including hemoglobin (Hgb), hematocrit (HCT), red blood cells (RBC), mean corpuscular volume (MCV), mean corpuscular hemoglobin (MCH), mean corpuscular hemoglobin concentration (MCHC), and red blood cell distribution width (RDW)). (D) Platelet indices. (E) Total number of bone marrow nucleated cells determined by trypan blue exclusion. Mean values and standard errors are shown (n=5-6 per group. *p<0.05, **p<0.01, ***p<0.001, NS = not significant, unpaired t-test).

Supplemental Figure 3

A

B

C

D

**Supplemental Figure 3: MRX-2843 increases ST-HSCs and reduces megakaryocyte-erythrocyte progenitors in C57BL/6 mice.** Wild-type, non-tumor bearing C57BL/6 mice were treated with 60mg/kg MRX-2843 once a day or an equivalent volume of vehicle (saline) administered by oral gavage for 24 days. Bone marrow was harvested from the femurs and tibia and progenitor populations were assessed using flow cytometry. (A) Representative flow cytometry profiles used to identify hematopoietic stem cells (HSC) and multipotent progenitors (MPP) in the bone marrow. The lineage negative LSK population was identified as $Lin^-Sca-1^+c-Kit^+$ cells. Within the LSK population, long-term hematopoietic stem cells (LT-HSC) were identified as $CD34^-Flk2^-$, short-term hematopoietic stem cells (ST-HSC) were identified as $CD34^+Flk2^-$, and the multipotent progenitor (MPP) population was identified as $CD34^+Flk2^+$. (B) Graphical representation of HSCs and MPP numbers. (C) Representative flow plots depicting the bone marrow progenitor populations. Top panels: Identification of $Lin^-Sca-1^-c-Kit^+$ populations. Bottom panels: Identification of myeloid progenitors. Within the $Lin^-Sca-1^-c-Kit^+$ populations, $CD127^-$ cells were defined as myeloid progenitors. Myeloid progenitors were further divided into subpopulations: common myeloid progenitors (CMP) were identified as $CD34^{dim}Fc\gamma R^{intermediate}$, granulocyte-monocyte progenitors (GMP) as $CD34^+Fc\gamma R^+$ and megakaryocyte-erythrocyte progenitors (MEP) as $CD34^-Fc\gamma R^-$. (E) Graphical representation of the $Lin^-Sca-1^-c-Kit^+$ progenitor, CMP, GMP and MEP populations. Mean values and standard errors are shown (n=6, *p<0.05, ***p<0.001, NS = not significant, unpaired t-test).

Supplemental Figure 4

A

B

C

D
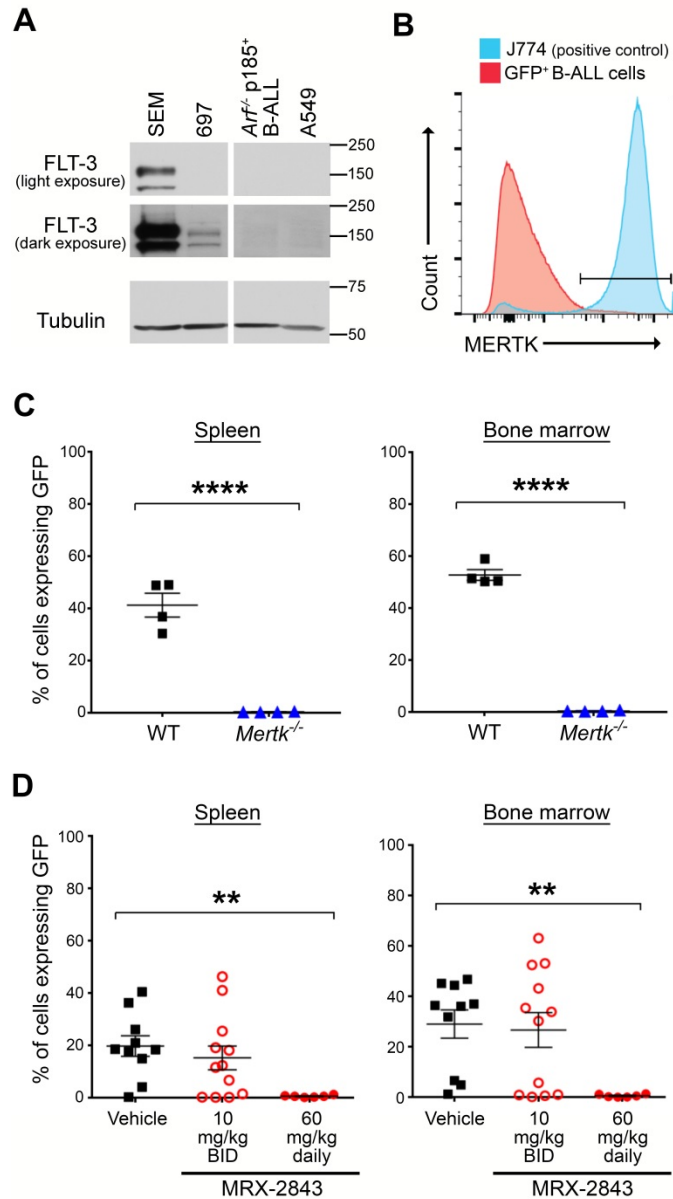
Supplemental Figure 4: MERTK inhibition reduces leukemic burden in a MERTK-negative, immune competent model of B-ALL. (A) FLT3 protein was detected in the indicated cell lines by immunoblot. The SEM cell line and tubulin are shown as positive and loading controls, respectively. (B) Bone marrow was collected from C57BL/6 mice 21 days after injection of 5×10^4 $Arf^{-/-}$ p185$^+$ B-ALL cells and MERTK expression was assessed by flow cytometry. Representative histograms from positive control cells (J774; blue line) and GFP$^+$ leukemia cells (red line) are shown (n=3). (C,D) C57BL/6 wild-type (WT) or $Mertk^{-/-}$ mice were injected intravenously with (C) 5×10^4 or (D) 5×10^3 $Arf^{-/-}$ p185$^+$ B-ALL cells. When symptoms of leukemia were evident in at least one mouse, bone marrow and spleens were harvested from those animals and their cagemates (one per group per cage) and stained for flow cytometric analysis. Leukemic burden was determined by measuring the percent GFP$^+$ cells in bone marrow and spleen. Mean values and standard errors from two independent cohorts are shown. (n=4-11, **$p<0.01$, ****$p<0.0001$ compared to WT or vehicle, 1-way ANOVA).
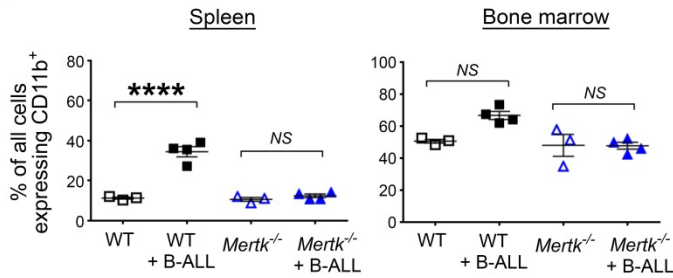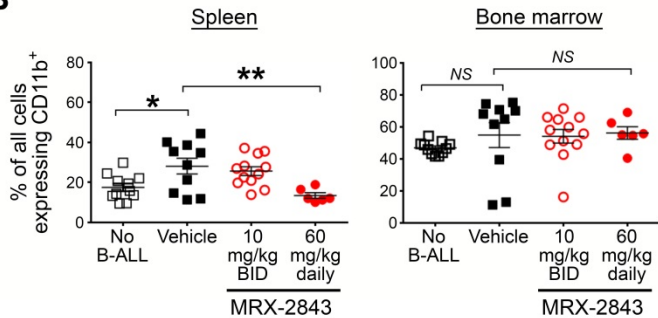
Supplemental Figure 5
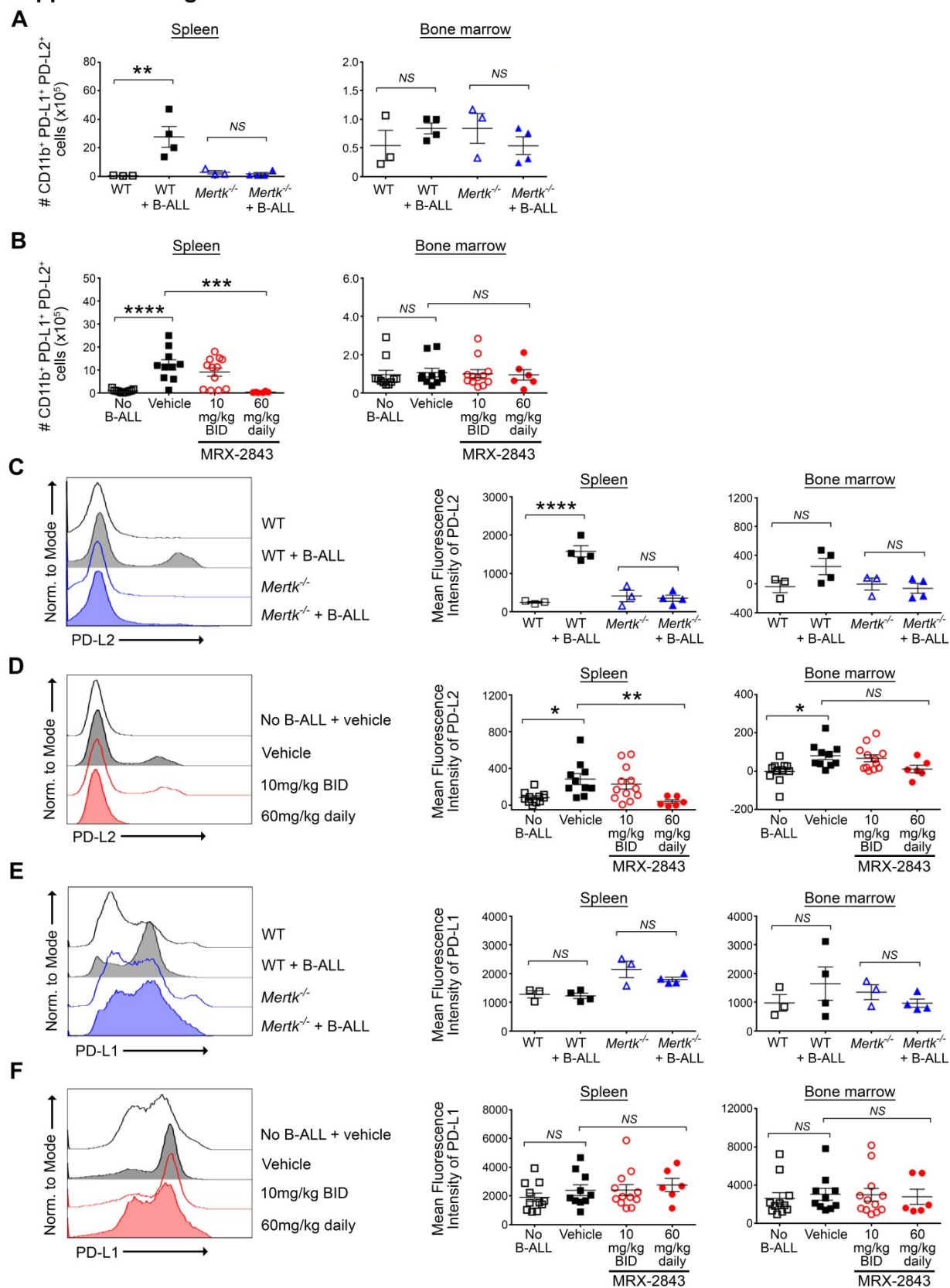
Supplemental Figure 5: MERTK inhibition alters co-inhibitory ligand and receptor expression in the leukemia microenvironment. C57BL/6 wild-type (WT) or *Mertk*$^{-/-}$ mice were injected with *Arf*$^{-/-}$ p185$^+$ B-ALL cells and treated as described in Figure 4. (A,B) Graphical representation of total numbers of GFP-negative CD11b$^+$ cells co-expressing PD-L1 and PD-L2 in spleens and marrow from (A) WT or *Mertk*$^{-/-}$ mice or (B) WT mice treated with MRX-2843 or vehicle. Mean values and standard errors from two independent cohorts are shown (n=3-11). (C-F) Representative histograms (left) and graphical representation (right) of PD-L1 or PD-L2 expression on CD11b$^+$ cell populations in spleens and marrow from mice with or without MERTK inhibition. (C) PD-L2 expression in wild-type or *Mertk*$^{-/-}$ mice. (D) PD-L2 expression in wild-type mice treated with MRX-2843 or vehicle. (E) PD-L1 expression in wild-type or *Mertk*$^{-/-}$ mice. (F) PD-L1 expression in wild-type mice treated with MRX-2843 or vehicle (saline). Mean values and standard errors derived from two independent cohorts are shown (n=3-11, *$p<0.05$, **$p<0.01$, ***$p<0.001$, ****$p<0.0001$, *NS* = not significant; 1-way ANOVA).

Supplemental Figure 6

A

Spleen — Bone marrow

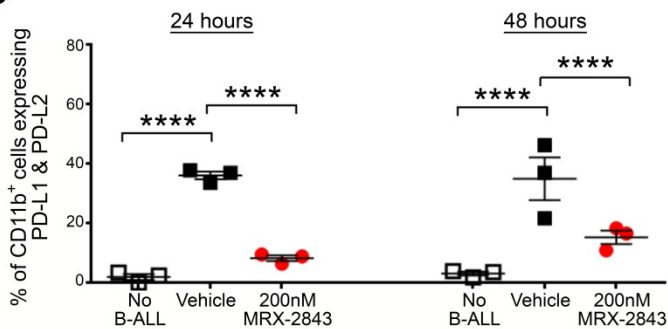**B**

Spleen — Bone marrow

C

24 hours — 48 hours

Supplemental Figure 6: MERTK inhibition increases splenic CD11b$^+$ cell populations in mice inoculated with leukemia and decreases co-expression of PD-L1 and PD-L2 on CD11b$^+$ myeloid cells *ex vivo*. (A-B) C57BL/6 wild-type (WT) or *Mertk$^{-/-}$* mice were injected with *Arf$^{-/-}$* p185$^+$ B-ALL cells and treated as described in Figure 4 (n=3-11 in two independent cohorts). (A) Graphical representation of total GFP-negative CD11b$^+$ cell populations in the spleen and marrow of WT or *Mertk$^{-/-}$* mice using flow cytometry. (B) Graphical representation of total GFP-negative CD11b$^+$ cell populations in the spleen and marrow using flow cytometry of WT mice treated with MRX-2843 or vehicle. (*$p<0.05$, **$p<0.01$, ****$p<0.0001$, NS = not significant; 1-way ANOVA). (C) Graphical representation of PD-L1/PD-L2 co-expressing GFP-negative CD11b$^+$ cells in *ex vivo* co-cultures. Splenocytes harvested from C57BL/6 mice were cultured in a 1:1 ratio with *Arf$^{-/-}$* p185$^+$ B-ALL cells and treated with 200nM MRX-2843 or vehicle for 24 or 48 hours, then PD-L1 and PD-L2 were assessed by flow cytometry. Mean values and standard errors from 3 independent experiments are shown. (****$p<0.0001$; 2-way ANOVA).
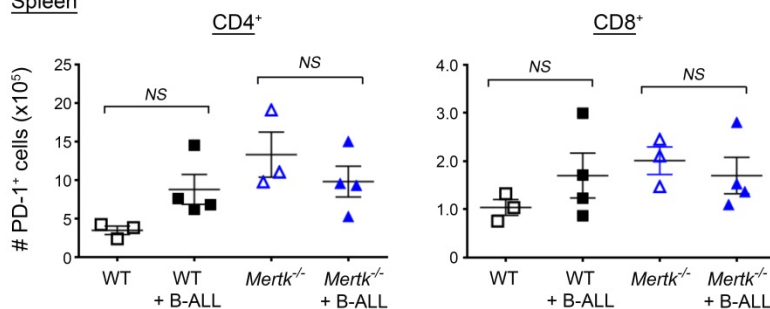
Supplemental Figure 7

A <u>Bone Marrow</u>

B <u>Bone Marrow</u>

C

D
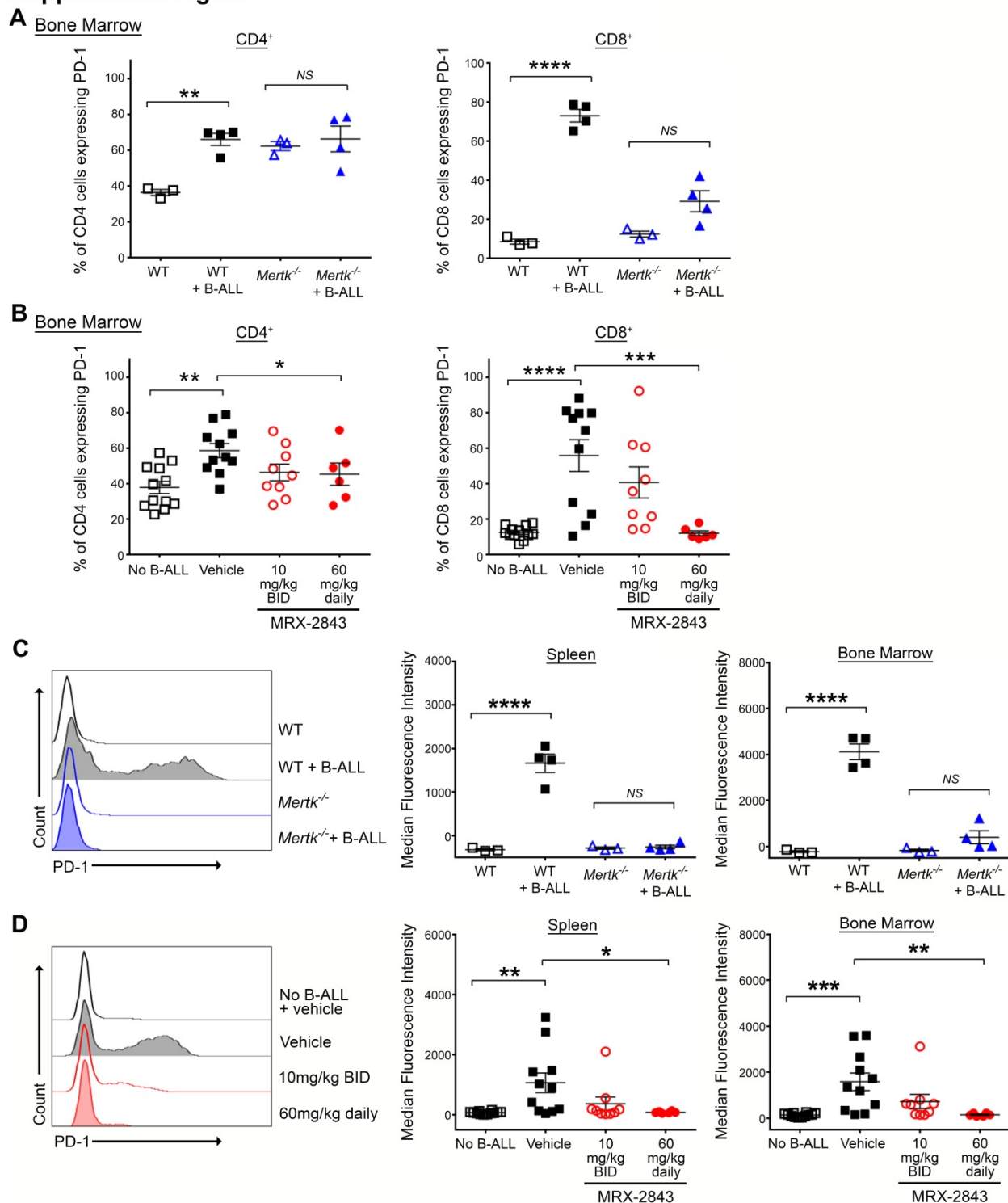
Supplemental Figure 7: MERTK inhibition reduces PD-1 expression on CD3$^+$ T cells in the leukemia microenvironment. C57BL/6 wild-type (WT) or *Mertk*$^{-/-}$ mice were treated as described in Figure 3 and spleen and marrow were evaluated by flow cytometry. (A) Percentages of PD-1$^+$ cells within the GFP$^-$ CD3$^+$ CD4$^+$ and CD8$^+$ populations in bone marrow

of WT and *Mertk*^{-/-} mice. (B) Percentages of PD-1$^+$ cells within the GFP$^-$ CD3$^+$ CD4$^+$ and CD8$^+$ population in bone marrow of WT mice treated with MRX-2843. (C) Left: Representative flow cytometry histograms demonstrating PD-1 expression on CD8$^+$ T cells within the GFP$^-$ CD3$^+$ population isolated from the spleen. Right: Graphical representation of the median fluorescence intensity of PD-1 expression in the GFP$^-$ CD3$^+$ CD8$^+$ population isolated from the spleen and marrow of WT or *Mertk*^{-/-} mice. (D) Left: Representative flow cytometry histograms demonstrating PD-1 expression on CD8$^+$ T cells within the GFP$^-$ CD3$^+$ population isolated from the spleen. Right: Graphical representation of the median fluorescence intensity of PD-1 expression in the GFP$^-$ CD3$^+$ CD8$^+$ population isolated from the spleen and marrow of WT mice treated with MRX-2843 or vehicle. Mean values and standard errors from two independent cohorts are shown. (n=3-12, **$p<0.01$, ***$p<0.001$, *NS*=not significant; 1-way ANOVA).
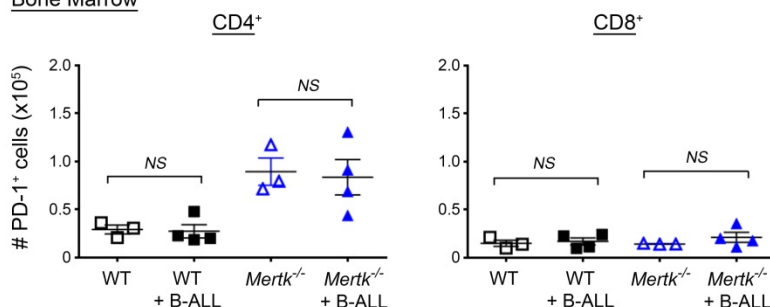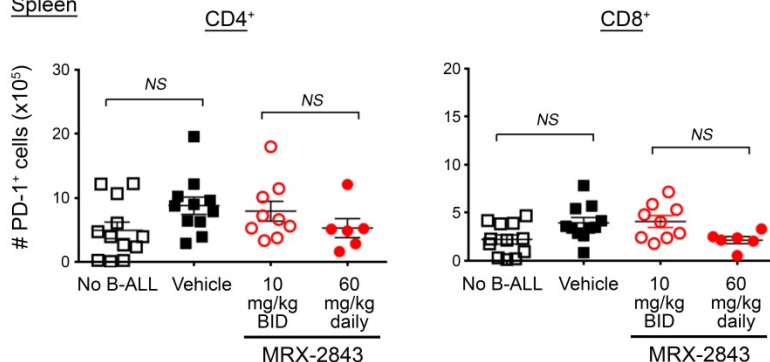
Supplemental Figure 8
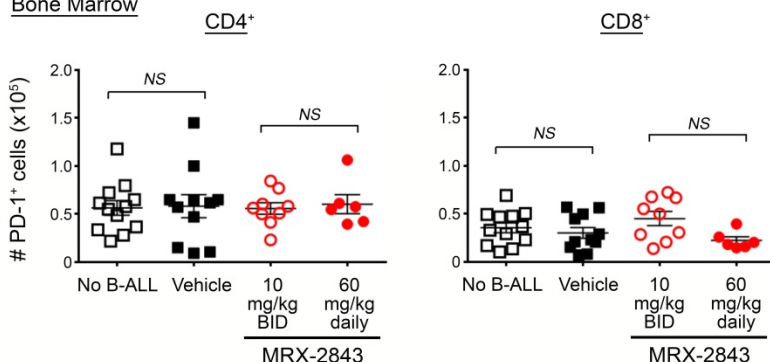
A Spleen

B Bone Marrow


C Spleen

D Bone Marrow

Supplemental Figure 8: Inoculation with leukemia and/or MERTK inhibition did not significantly impact total numbers of PD-1 expressing T cells in spleen and bone marrow. C57BL/6 wild-type (WT) or *Mertk*$^{-/-}$ mice were treated as described in Figure 4 and spleen and marrow were evaluated by flow cytometry. (A,B) Graphical representation of total GFP$^-$ CD4$^+$ and CD8$^+$ T cell numbers in spleens (A) or bone marrow (B) from WT or *Mertk*$^{-/-}$ mice.(C,D) Graphical representation of total GFP$^-$CD4$^+$ and CD8$^+$ T cell populations in spleens (C) or bone marrow (D) from WT mice treated with MERTK inhibitor MRX-2843 or saline vehicle. Mean values and standard errors from two independent cohorts are shown. (n=3-12, *NS*=not significant, 1-way ANOVA).

Supplemental Figure 9
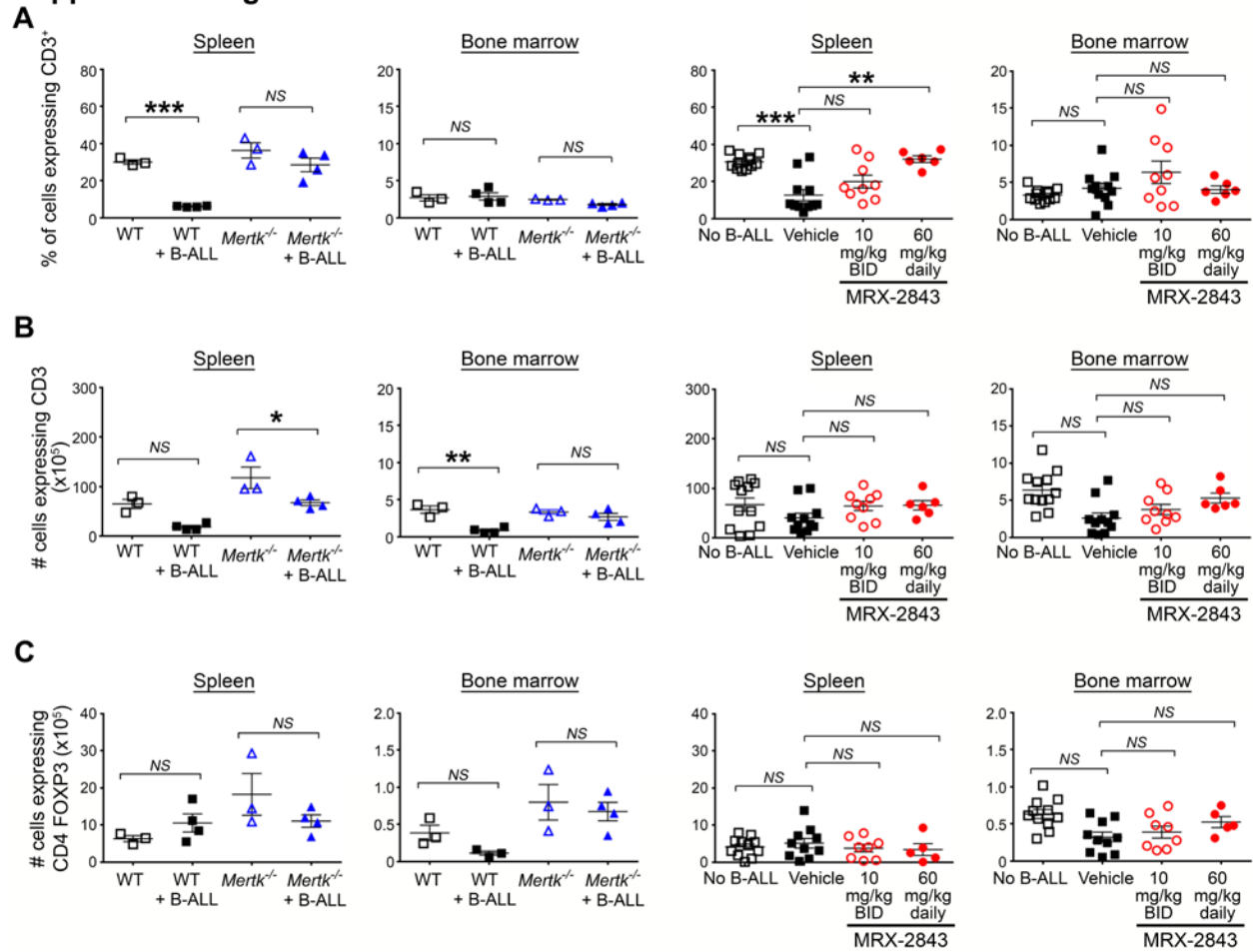
Supplemental Figure 9: MERTK inhibition increases the fraction of splenic CD3$^+$ T cells in mice inoculated with leukemia independent of changes in total numbers of T cells and T regulatory cells. C57BL/6 wild-type (WT) or *Mertk*$^{-/-}$ mice were treated as described in Figure 4 and spleen and marrow were evaluated by flow cytometry. Graphical representation of the (A) proportion of GFP$^-$ CD3$^+$ T cells, (B) total number of GFP$^-$ CD3$^+$ T cells, and (C) total number of GFP$^-$ CD4$^+$ FOXP3$^+$ cells in spleens and marrow from WT or *Mertk*$^{-/-}$ mice (left panels), or WT mice treated with MRX-2843 or saline vehicle (right panels). Mean values and standard errors derived from two independent cohorts are shown. (n=3-12, *p<0.05, **p<0.01, ***p<0.001 compared to vehicle, *NS*=not significant, 1-way ANOVA).